

Journal Pre-proof

Satellite-based assessment of mining-related sediment influence on water quality in an extractive river basin

Vincent Adjei, Lawson Mensah, Alex Owusu Amoakoh, Mary Antwi, Gideon Nkrumah, Isaac Stanislav Essah, Frederick Gyan, Vera Aseye Etor, Godfred Adu Boateng



PII: S0013-9351(26)00707-3
DOI: <https://doi.org/10.1016/j.envres.2026.124376>
Reference: YENRS 124376

To appear in: *Environmental Research*

Received date: 4 February 2026
Revised date: 24 March 2026
Accepted date: 26 March 2026

Please cite this article as: V. Adjei, L. Mensah, A.O. Amoakoh et al., Satellite-based assessment of mining-related sediment influence on water quality in an extractive river basin. *Environmental Research* (2026), doi: <https://doi.org/10.1016/j.envres.2026.124376>.

This is a PDF of an article that has undergone enhancements after acceptance, such as the addition of a cover page and metadata, and formatting for readability. This version will undergo additional copyediting, typesetting and review before it is published in its final form. As such, this version is no longer the Accepted Manuscript, but it is not yet the definitive Version of Record; we are providing this early version to give early visibility of the article. Please note that Elsevier's sharing policy for the Published Journal Article applies to this version, see: <https://www.elsevier.com/about/policies-and-standards/sharing#4-published-journal-article>. Please also note that, during the production process, errors may be discovered which could affect the content, and all legal disclaimers that apply to the journal pertain.

© 2026 Published by Elsevier Inc.

1 Highlights

2 **Satellite-based assessment of mining-related sediment influence on** 3 **water quality in an extractive river basin**

4 Vincent Adjei^{}, Lawson Mensah^{}, Alex Owusu Amoakoh^{}, Mary Antwi^{},
5 Gideon Nkrumah, Isaac Stanislav Essah^{}, Frederick Gyan, Vera Aseye Etor,
6 Godfred Adu Boateng^{}

- 7 • Multi-decadal satellite analysis reveals substantial land-cover transi-
8 tions in a mineralised river basin.
- 9 • Mining-related land disturbance is a dominant driver of sediment-related
10 water-quality degradation.
- 11 • Degradation of water quality is spatially clustered, indicating hotspot-
12 driven rather than basin-wide pressure.
- 13 • Integration of satellite-derived land cover and field measurements strength-
14 ens spatial assessment of land-use influences on water quality.
- 15 • Linking land-use composition with water-quality variation supports
16 more targeted environmental management.

17 Satellite-based assessment of mining-related sediment
 18 influence on water quality in an extractive river basin

19 Vincent Adjei^a, Lawson Mensah^a, Alex Owusu Amoakoh^{b,c,*}, Mary
 20 Antwi^d, Gideon Nkrumah^a, Isaac Stanislav Essah^e, Frederick Gyan^a,
 21 Vera Aseye Ekor^a, Godfred Adu Boateng^f

^a*Department of Environmental Science, College of Science, Kwame Nkrumah University
 of Science and Technology, Kumasi, AR, Ghana*

^b*Liverpool Research Institute for Climate and Sustainability (LiRICS), Liverpool John
 Moores University, Byrom Street, Liverpool, L3 3AF, United Kingdom*

^c*Natural Capital Hub, School of Biological and Environmental Sciences, Faculty of
 Science, Liverpool John Moores University, Liverpool, United Kingdom*

^d*Department of Environmental Management, School of Natural Resources, University of
 Energy and Natural Resources, Sunyani, BA, Ghana*

^e*Department of Wildlife and Range Management, Faculty of Renewable Natural
 Resources, College of Agriculture and Natural Resources, Kwame Nkrumah University of
 Science and Technology, Kumasi, AR, Ghana*

^f*Department of Geography and Regional Planning, University of Cape Coast, Cape
 Coast, CR, Ghana*

22 **Abstract**

Extractive activities drive land transformation in many mineralised river basins. However, linking these changes to observable and attributable water-quality outcomes remains methodologically challenging. This study applies an integrated monitoring framework to examine how multi-decadal Land-use and land-cover change (LULC) translates into spatially differentiated river water quality in the Ankobra River basin, Ghana. Using harmonised Landsat and Sentinel imagery, LULC dynamics was reconstructed for 1986, 2002, 2016, and 2025. Field-based measurements of key physico-chemical water-quality parameters were collected to support the analysis. Spatial interpolation using Ordinary Kriging and redundancy analysis was then applied to assess the extent to which land-use composition explains the observed variation in water quality. The results showed a shift from forest-dominated land cover towards agriculture, settlement, and mining-related disturbance during the study period. Bareland/Mining expanded from less than 1% of the basin in 1986 to approximately 3.7% by 2025 (>100 km²), while combined

*Corresponding author: Alex Owusu Amoakoh (email: a.o.amoakoh@ljmu.ac.uk)

forest cover declined overall throughout the study period. Water-quality patterns exhibited strong spatial gradients, with turbidity ranging from approximately 114 to more than 1000 NTU and total suspended solids (TSS) from around 100 to nearly 3000 mg L⁻¹. Redundancy analysis indicated that land-use composition explained approximately 47.5% of the variance in water quality, with the mining-related land cover exerting the strongest influence ($F = 13.66$, $p < 0.001$) and showing robust positive associations with turbidity and TSS. Closed forest cover displayed a significant buffering effect, while agricultural land use did not show significant association on the spatial scale examined. These findings demonstrate how integrated Earth observation and field data can move sustainability assessment beyond descriptive convergence towards diagnostic clarity. The analytical framework offers a transparent and scalable approach for prioritising regulatory attention and monitoring in extractive landscapes where environmental pressures are spatially uneven and governance capacity is constrained.

23 *Keywords:* Land-use change, Mining disturbance, Machine learning,
24 Sediment dynamics, Sustainability assessment

25 **1. Introduction**

26 Extractive activities continue to play a central role in economic development
27 in many low- and middle-income countries, yet their environmental and social
28 sustainability remains persistently contested. Large-scale artisanal mining
29 operations frequently generate extensive land disturbance, alter hydrologi-
30 cal pathways, and introduce sediments and contaminants into river systems,
31 with consequences that extend well beyond the immediate footprint of ex-
32 traction (Bebbington et al., 2018; Hilson et al., 2020; Obodai et al., 2019).
33 In West Africa, and especially Ghana, artisanal gold mining (ASM) has been
34 associated with widespread river turbidity, sediment mobilisation, and chan-
35 nel modification in major basins, including Pra, Offin, Ankobra, and Birim
36 (Hilson, 2002; Kuma and Younger, 2004; Obodai et al., 2019). These im-
37 pacts shape biophysical conditions, livelihoods, regulatory legitimacy, and
38 longer-term development trajectories, particularly in regions where rivers un-
39 derpin domestic water supply, agriculture, and ecosystem services. In such
40 settings, sustainability cannot be meaningfully assessed by production met-
41 rics or formal compliance reporting alone. It requires integrated evidence
42 that links land-use change with observable environmental outcomes within

43 affected river basins.

44 Despite this need, sustainability assessment in extractive landscapes re-
45 mains fragmented. Land use dynamics is commonly monitored using satel-
46 lite Earth observation, while water quality is assessed through field sampling
47 campaigns that are often spatially limited and temporally discontinuous (Al-
48 lan et al., 2017). Remote sensing can document the expansion and contrac-
49 tion of mining, agriculture, and settlement over time; however, it does not
50 directly indicate how such changes translate into aquatic system degradation.
51 In contrast, water-quality measurements can identify elevated turbidity, sus-
52 pended solids, or dissolved constituents, but lack the spatial context required
53 to attribute these conditions to specific land-use pressures. As a result, reg-
54 ulators and planners are often left with parallel strands of evidence that are
55 difficult to reconcile, constraining the transition from environmental diagno-
56 sis to sustainability-oriented decision-making.

57 Recent advances in cloud-based geospatial platforms and analytical meth-
58 ods offer new opportunities to address these challenges, but their application
59 in extractive contexts remains uneven. Long-term satellite archives, includ-
60 ing Landsat and Sentinel, now support consistent reconstruction of land-
61 cover trajectories over several decades, while machine-learning classifiers have
62 improved mapping reliability in heterogeneous tropical environments (e.g.,
63 Gorelick et al., 2017; Belgiu and Drăguț, 2016; Amoakoh et al., 2024, 2021).
64 At the same time, spatial statistical techniques enable the visualisation of
65 basin-scale gradients in water-quality parameters derived from discrete sam-
66 pling observations, allowing environmental patterns to be examined spatially
67 (Li and Heap, 2014). What remains less well developed is the use of these
68 tools to support explicit attribution of water-quality variation to dominant
69 land-use pressures in mineralised river basins. In Ghana, most mining-water
70 studies rely on point-based sampling designs that document contamination,
71 but do not systematically integrate long-term land-cover trajectories derived
72 from satellite archives (e.g., Obodai et al., 2019; Armah et al., 2010; Duncan
73 et al., 2018). Therefore, while degradation is well documented, spatial at-
74 tribution of river condition to specific land-use transitions remains limited.
75 Integrated analyses consequently remain largely descriptive, demonstrating
76 co-occurrence between land-use change and water-quality decline without
77 providing the diagnostic evidence needed to prioritise regulatory action or
78 inform sustainability governance.

79 This study applies an integrated monitoring framework to the Anko-
80 bra Basin, Ghana, linking multi-decadal LULC dynamics with spatially dis-

81 tributed water-quality observations in an extractive landscape. The aim is
82 to assess how contemporary land-use composition explains spatial variation
83 in river water quality measured within a landscape shaped by multi-decadal
84 transformation. Specifically, the study (i) reconstructs multi-decadal LULC
85 trajectories in a mineralised river basin using satellite Earth observation data;
86 (ii) characterises the spatial variability of key water-quality parameters based
87 on field measurements, supported by spatial visualisation; and (iii) evaluates
88 the extent to which contemporary land-cover composition explains observed
89 spatial variation in water-quality parameters, with emphasis on sediment-
90 related indicators. In doing so, the study adopts an attribution-oriented
91 analytical framework aimed at improving transparency and diagnostic clar-
92 ity in the assessment of sustainability (Scoones, 2016; Newell, 2019; Turnhout
93 et al., 2020).

94 **2. Methodology**

95 *2.1. Study area*

96 The study was conducted in the Ankobra River basin, located in south-
97 western Ghana, and covers approximately 2892 km² in Prestea–Huni Valley
98 (PHV) and Nzema East (NE) districts of the Western Region (Figure 1).
99 The Ankobra river flows south before discharging into the Gulf of Guinea at
100 Sanwoma. Prestea–Huni Valley district occupies approximately 1809 km² of
101 the basin and is characterised by undulating terrain and a long history of
102 industrial and artisanal gold mining centred around Bogoso (Opoku et al.,
103 2017; Wiafe et al., 2022). The NE district covers approximately 1083 km² of
104 the basin.

105 The area experiences a humid equatorial climate with bimodal rainfall
106 ranging from approximately 1500 to 2000 mm annually (Cudjoe et al., 2023).
107 Vegetation transitions from moist semi-deciduous forests in the northern part
108 of the basin to secondary forests and coastal savannahs in the south, inter-
109 spersed with forest reserves and extensive rubber and cocoa plantations (Obo-
110 dai et al., 2019). Economic activities are dominated by agriculture, mining,
111 forest management and fishing, resulting in sustained anthropogenic pressure
112 on riparian zones and forest ecosystems. The basin contains multiple licensed
113 mining concessions (Figure 1), reflecting its role in Ghana’s gold production
114 corridor. Documented multi-decadal expansion of mining-related disturbance
115 and forest-to-agriculture transitions in both districts creates marked spatial

116 heterogeneity in land-use composition (e.g., Amoakoh et al., 2021, 2024; Obo-
 117 dai et al., 2019). These characteristics make the Ankobra basin a suitable
 118 case for examining how cumulative land-use change influences spatial varia-
 119 tion in river water quality within an extractive landscape.

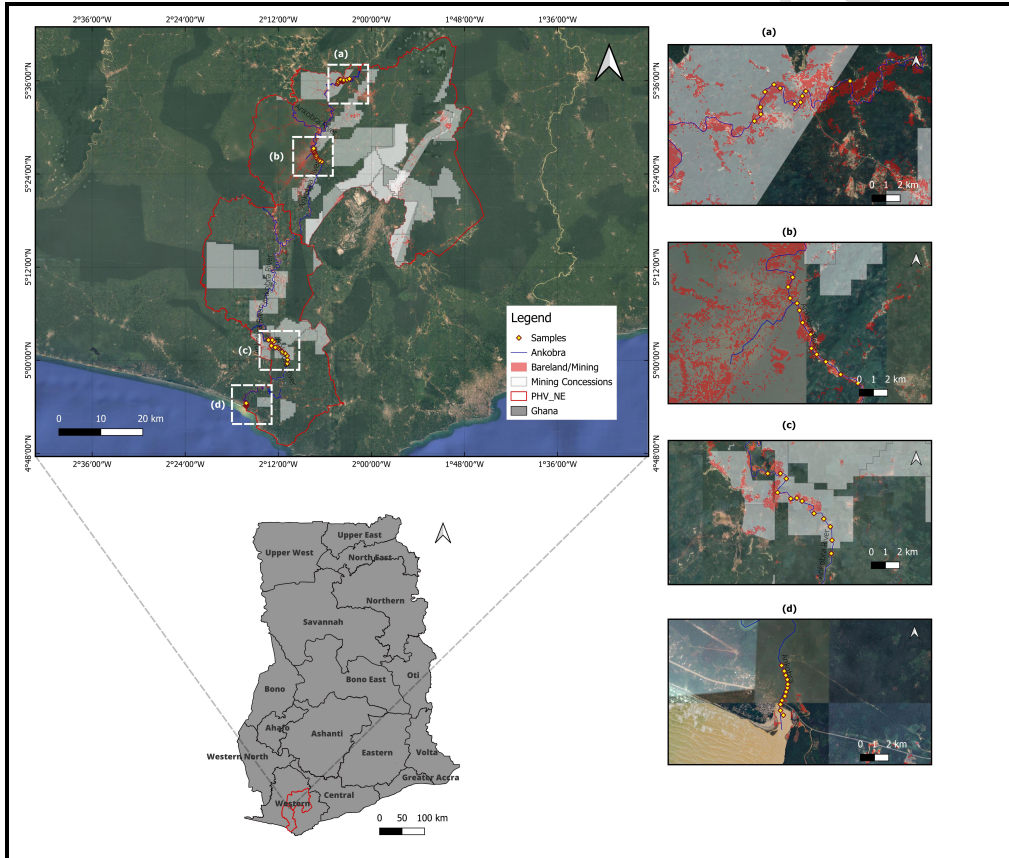


Figure 1: Study area map of the Ankobra River Basin showing the Prestea–Huni Valley (PHV) and Nzema East (NE) districts. The map displays water-quality sampling locations, the Ankobra River network, 2025 Bareland/Mining areas derived from the land-cover classification, and licensed mining concession boundaries obtained from the Ghana Mining Repository (Minerals Commission of Ghana, n.d.). Insets (a–d) provide detailed views of selected river reaches and sampling points. Basemap imagery © Google.

120 *2.2. Satellite data and pre-processing*

121 Multi-temporal satellite imagery was used to analyse the LULC dynamics at
122 four time points that represent long-term change in the basin (Table 1). Sur-
123 face reflectance products, from Landsat and Sentinel missions were accessed
124 via the Google Earth Engine (GEE) cloud platform (Google LLC, Moun-
125 tain View, California, USA), which provides consistent pre-processing and
126 facilitates temporal compositing at basin scale (Gorelick et al., 2017). Land-
127 sat data were obtained from the United States Geological Survey (USGS)
128 archive, including Landsat 5 Thematic Mapper (TM) imagery for 1986 and
129 Landsat 7 Enhanced Thematic Mapper Plus (ETM+) imagery for 2002.
130 Sentinel-2 Multispectral Instrument (MSI) imagery for 2016 and 2025 was
131 provided by the European Space Agency (ESA). These time points were se-
132 lected to capture pre-intensification, transition, and recent phases of land-use
133 change, while ensuring sufficient cloud-free observations for reliable composit-
134 ing in a persistently cloudy tropical environment. Sentinel-2 MSI imagery
135 was used for the later time points due to its availability during the most recent
136 period and its high revisit frequency, which improves the likelihood of ob-
137 taining cloud-free observations in humid tropical environments. To minimise
138 atmospheric effects and data gaps, annual image composites were generated
139 using scenes with less than 10% cloud cover. Cloud-affected pixels were
140 removed using the GEE cloud probability masking approach, and median
141 composites were produced to reduce residual noise. This approach ensured
142 temporal comparability across years while maximising spatial coverage for
143 classification.

144 All satellite images were harmonised to a common spatial resolution prior
145 to classification. Sentinel-2 MSI bands were resampled at 30 m to match the
146 native spatial resolution of the Landsat imagery. This resolution was selected
147 to preserve comparability across the full temporal range of the analysis while
148 avoiding artificial inflation of spatial detail in earlier years. Resampling was
149 performed using a bilinear interpolation approach for continuous spectral
150 bands, which minimises aliasing effects and preserves radiometric continuity
151 relative to nearest-neighbour methods (Jensen, 2016).

152 *2.3. Land Cover Classification*

153 Supervised classification was applied to the annual composites to derive
154 LULC maps for each study year. Standard spectral band combinations,
155 including natural colour, false colour infrared, and shortwave infrared–near

Table 1: Satellite imageries used for LULC analysis

Year	Satellite	Spatial resolution (m)
1986	Landsat 5 TM	30
2002	Landsat 7 ETM+	30
2016	Sentinel-2 MSI (L1C)	10, 20, 60
2025	Sentinel-2 MSI (L2A)	10, 20, 60

156 infrared composites, were used to support visual interpretation and train-
 157 ing sample selection. A Random Forest classifier was implemented within
 158 Google Earth Engine due to its robustness to non-linear relationships and its
 159 demonstrated performance in heterogeneous tropical landscapes (Amoakoh
 160 et al., 2021).

161 Six LULC classes were defined based on dominant land-use characteristics
 162 and spectral similarity within the basin: water, bareland/mining, settlement,
 163 agriculture, closed forest and open forest (Table 2). Mining pits and other
 164 exposed surfaces were grouped under a single Bareland/Mining class due to
 165 their similar spectral reflectance characteristics. The class captures surface
 166 conditions associated with gold extraction, including both industrial and ar-
 167 tisanal operations, without differentiating between mining types. Although
 168 bare ground and mining pits are functionally distinct land uses, aggregation
 169 was adopted to represent sediment-relevant exposure at 30 m resolution.
 170 Therefore, the class does not correspond directly to the formally delineated
 171 concession boundaries (see Figure 1) and may marginally overestimate the
 172 footprint of active mining areas. Dense cocoa farms, mature rubber planta-
 173 tions, and intact forest were operationally classified as Closed Forest based
 174 on high canopy density, while areas of sparse vegetation, fallow land, shrubs,
 175 and young plantations were classified as Open Forest to represent low vege-
 176 tation cover.

177 Training samples for the 2025 classification were derived from field-verified
 178 coordinates and high-resolution reference imagery. These samples were trans-
 179 ferred to earlier years through visual interpretation of historical imagery to
 180 ensure temporal consistency in class definitions across the study period.

181 *2.4. Post classification change analysis and accuracy assessment*

182 Post-classification change detection was conducted to quantify transitions be-
 183 tween LULC classes over three periods: 1986–2002, 2002–2016, and 2016–2025.
 184 Cross-tabulation matrices were generated using TerrSet 19.0.6 (Clark Labs,

Table 2: Description of LULC classes

LULC class	Description
Water	Rivers and water-filled mining pits
Bareland/Mining	Mining-disturbed surfaces and exposed bare ground
Settlement	Buildings, developed areas, and impervious surfaces
Agriculture	Croplands and farmlands
Closed Forest	Dense forest and high-canopy plantations
Open Forest	Sparse vegetation, shrubs, and fallow land

185 Clark University, USA) to calculate area changes and transition patterns, al-
 186 lowing the identification of dominant land-cover conversions over time. The
 187 classification accuracy was assessed using confusion matrices derived from
 188 independent validation samples. Overall accuracy, precision, recall, and F1-
 189 score were computed using GEE's built-in accuracy assessment functions,
 190 following standard definitions (Allan, 2004):

$$\text{Overall Accuracy} = \frac{\text{Number of correctly classified pixels}}{\text{Total number of pixels}} \times 100 \quad (1)$$

$$\text{Precision} = \frac{TP}{TP + FP} \quad (2)$$

$$\text{Recall} = \frac{TP}{TP + FN} \quad (3)$$

$$\text{F1-score} = 2 \times \frac{\text{Precision} \times \text{Recall}}{\text{Precision} + \text{Recall}} \quad (4)$$

191 where TP (true positives) represents correctly classified pixels for a given
 192 LULC class, FP (false positives) represents pixels incorrectly assigned to
 193 that class, and FN (false negatives) represent pixels belonging to that class
 194 that were incorrectly assigned to another class.

195 2.5. Water-quality data collection and analysis

196 Water-quality sampling followed a stratified design that combined the pur-
 197 positive delineation of the river reaches with random sampling within each
 198 stratum. The river was divided into four reaches that represent upstream
 199 and downstream conditions, as well as the spatial distribution of dominant

200 land-use pressures within the study area. Within each reach, water samples
 201 were collected at randomly selected locations along the river, yielding a total
 202 of 48 samples in all strata. Candidate sampling locations were generated
 203 using a random point algorithm constrained to the river polyline within each
 204 reach in ArcGIS (Esri Inc., Redlands, California, USA). Where randomly
 205 generated locations were inaccessible due to terrain or safety constraints, the
 206 nearest accessible point within a short upstream or downstream tolerance
 207 was sampled. This preserved random allocation while accommodating prac-
 208 tical field constraints and minimising systematic accessibility bias. Sampling
 209 was conducted between January and February 2025, during the peak dry
 210 season in southwestern Ghana, reducing short-term rainfall-driven variabil-
 211 ity and facilitating clearer identification of spatial contrasts associated with
 212 near-stream land-use pressures.

213 In situ measurements of turbidity, pH, dissolved oxygen (DO), electri-
 214 cal conductivity (EC), and total dissolved solids (TDS) were obtained us-
 215 ing a HANNA HI 9829 multiparameter probe (Hanna Instruments Inc.,
 216 Woonsocket, Rhode Island, USA). For total suspended solids (TSS) analysis,
 217 water samples were collected in 500 mL high-density polyethylene bottles
 218 and transported in an icebox at temperatures below 4 °C prior to laboratory
 219 (Adusei et al., 2021). Laboratory determination of TSS was conducted using
 220 the DR3900 Spectrophotometer (Hach Company, Loveland, Colorado, USA).

221 Spatial patterns of the water-quality parameters were estimated using
 222 Ordinary Kriging based on euclidean distance in ArcGIS 10.8. This method
 223 was selected because it explicitly accounts for spatial autocorrelation and
 224 is suitable for datasets where sampling points are unevenly distributed or
 225 clustered (Osei et al., 2024). A spherical semivariogram model was specified
 226 within the ArcGIS Kriging tool. The interpolation assumed isotropic spatial
 227 dependence and did not explicitly model nested spatial structures, reflecting
 228 the moderate sample density and linear distribution of sampling points along
 229 the river corridor. The method estimates unknown values as a weighted linear
 230 combination of observed samples (5):

$$Z^*(x) = \sum_{i=1}^n \lambda_i Z(x_i) \quad (5)$$

231 where λ_i are the kriging weights and $Z(x_i)$ represents the observed values at
 232 sampled locations. The resulting interpolated surfaces were used to visualise
 233 spatial variability in water-quality conditions and to identify areas of elevated

234 environmental pressure within the basin.

235 *2.6. Linking land use and water quality through redundancy analysis*

236 Redundancy analysis (RDA) was employed to examine the extent to which
 237 spatial variation in water-quality parameters could be explained by surround-
 238 ing land-use composition. RDA is a constrained ordination technique that
 239 combines multiple regression with principal component analysis, allowing di-
 240 rect assessment of relationships between explanatory and response variables
 241 (Ma et al., 2025). For each sampling location, land-use composition was
 242 quantified as the percentage cover of each LULC class within a 250 m buffer
 243 derived from the 2025 land-cover map. The buffer was defined to represent
 244 the direct influence of the riparian and near-channel land-uses. In humid
 245 tropical systems, sediment mobilisation is strongly mediated by disturbance
 246 within immediate stream corridors, where vegetation removal and soil ex-
 247 posure enhance delivery to adjacent channels (Naiman and Decamps, 1997;
 248 Dosskey et al., 2010). Although sediment processes operate at broader catch-
 249 ment scales, the analysis was designed to capture land-use pressures proximal
 250 to sampling locations rather than to model full watershed dynamics.

251 The water-quality parameters measured at the same locations were stan-
 252 dardised prior to analysis to ensure comparability. In matrix form, RDA can
 253 be expressed as a multivariate linear model of the form:

$$\mathbf{Y} = \mathbf{XB} + \mathbf{E} \quad (6)$$

254 where \mathbf{Y} is the matrix of standardised water-quality response variables, \mathbf{X} is
 255 the matrix of land-use explanatory variables, \mathbf{B} is the matrix of regression
 256 coefficients, and \mathbf{E} represents residual variation not explained by land use.

257 The RDA was implemented in R using the vegan package (version 2.7-
 258 2), with LULC classes specified as explanatory variables and water-quality
 259 parameters as response variables. Statistical significance was assessed using
 260 Monte Carlo permutation tests, enabling the evaluation of whether the ob-
 261 served relationships differed from those expected by chance. This provided
 262 a statistically grounded basis for assessing the extent to which the current
 263 (2025) land-use composition explains the observed spatial variation in water-
 264 quality parameters within the extractive landscape.

265 3. Results

266 3.1. LULC dynamics

267 LULC analysis revealed substantial spatial and temporal change in the Anko-
268 bra River basin between 1986 and 2025 (Figure 2; Table 3). In 1986, the
269 basin was predominantly characterised by Closed Forest and Open Forest
270 classes, which together covered more than half of the basin area, reflecting
271 relatively intact forest cover. Agricultural land occupied a smaller propor-
272 tion of the landscape, while Bareland/Mining and Settlement each accounted
273 for less than 5% of total land cover. Between 1986 and 2002, the most pro-
274 nounced changes were associated with the expansion of agricultural land and
275 Bareland/Mining areas, particularly within the Prestea–Huni Valley district.
276 Agricultural land approximately doubled in extent during this period, while
277 forest cover declined through transitions mainly from Closed Forest to Open
278 Forest and Agriculture (Table 3, Appendix A2). The expansion of Settlement
279 remained spatially concentrated around existing urban centers and transport
280 corridors and increased substantially between 2002 and 2016; however, its
281 proportional contribution to total basin area remained smaller than agricul-
282 ture and forest transitions.

283 Between 2002 and 2016, Bareland/Mining expanded sharply, increasing
284 by more than an order of magnitude compared to 1986, exceeding 100 km²
285 by 2025 (Figure 2). This expansion coincided with continued net losses in
286 both closed and open forest classes. Agricultural land continued to expand,
287 although at a slower rate relative to mining-related disturbances, while Set-
288 tlement growth became more spatially evident, reflecting increased urbanisa-
289 tion and infrastructure development. The dynamics between 2016 and 2025
290 continued to reflect a strong anthropogenic influence, particularly through
291 the further expansion of bareland/mining, which increased substantially to
292 exceed 100 km² by 2025 (Figure 2). In contrast, Agricultural land declined
293 relative to 2016 levels, while both closed forest and open forest classes exhib-
294 ited moderate increases. The extent of settlement remained broadly stable
295 during this period (Figure3).

Table 3: LULC area statistics for the Ankobra River basin (km² and %)

LULC class	1986		2002		2016		2025	
	Area (km ²)	%						
Water	19.99	0.69	13.17	0.46	19.76	0.68	10.90	0.38
Bareland/Mining	3.07	0.11	4.96	0.17	30.46	1.05	107.96	3.73
Settlement	28.21	0.98	21.39	0.74	146.91	5.08	148.38	5.13
Closed Forest	1092.07	37.76	948.74	32.81	904.48	31.27	932.86	32.26
Open Forest	1482.34	51.26	1369.89	47.37	1114.11	38.53	1192.72	41.24
Agriculture	266.34	9.21	533.86	18.46	676.08	23.38	499.12	17.26
Total	2892.02		2892.01		2891.80		2891.94	

296 *3.2. Accuracy assessment of land-cover classification*

297 Overall classification accuracy ranged from 81% to 92% during the study
298 period (Table 4). At the class level, Water, Closed Forest, and Open Forest
299 were generally well classified across all years, with F1-scores ranging from
300 0.84 to 0.94 (Table 4). Classification performance for Bareland/Mining and
301 Settlement exhibited greater variability, particularly in earlier years, with F1-
302 scores between 0.76 and 0.83, reflecting spectral similarity to other exposed
303 or impervious surfaces. Classification performance for these classes improved
304 in 2025, with F1-scores approaching 0.90, indicating improved discrimination
305 in the higher-resolution Sentinel-2 data.

306 *3.3. Spatial patterns of water-quality parameters*

307 Turbidity and total suspended solids (TSS) exhibited elevated concentra-
308 tions in river sections downstream of major mining areas, particularly within
309 the Prestea–Huni Valley district (Figure 4). Turbidity values ranged from
310 approximately 114 to over 1000 NTU, while TSS concentrations varied be-
311 tween 101 and nearly 3000 mg L⁻¹, with elevated values occurring in spatially
312 clustered segments rather than uniformly along the river network. Electric-
313 al conductivity (EC) and total dissolved solids (TDS) displayed increasing
314 trends towards the lower reaches of the basin, especially near the coastal
315 zone. EC values ranged from approximately 65 $\mu\text{S cm}^{-1}$ upstream to over
316 12,000 $\mu\text{S cm}^{-1}$ near the estuary, while TDS concentrations varied from below
317 100 mg L⁻¹ in upstream sections to values exceeding 6000 mg L⁻¹ in down-
318 stream reaches (Figure 4). Dissolved oxygen (DO) concentrations showed
319 moderate spatial variability, ranging from approximately 4.6 to 6.8 mg L⁻¹,
320 with lower values observed in river segments adjacent to intensive land distur-
321 bance. In contrast, pH values varied within a relatively narrow range, from
322 approximately 5.2 to 6.8, indicating generally acidic to near-neutral condi-
323 tions across the basin. Summary statistics for all water-quality parameters
324 are provided in Table 5.

325 *3.4. Relationships between land use and water quality*

326 The redundancy analysis (RDA) showed that land-use composition explains a
327 substantial proportion of the observed variation in water-quality parameters.
328 The constrained model was statistically significant ($F = 6.95$, $p < 0.001$),
329 accounting for approximately 47.5% of the total variance in water quality
330 (Figure 5). The first canonical axis (RDA1) accounted for 44.2% of the
331 constrained variance, capturing the dominant land-use gradient structuring

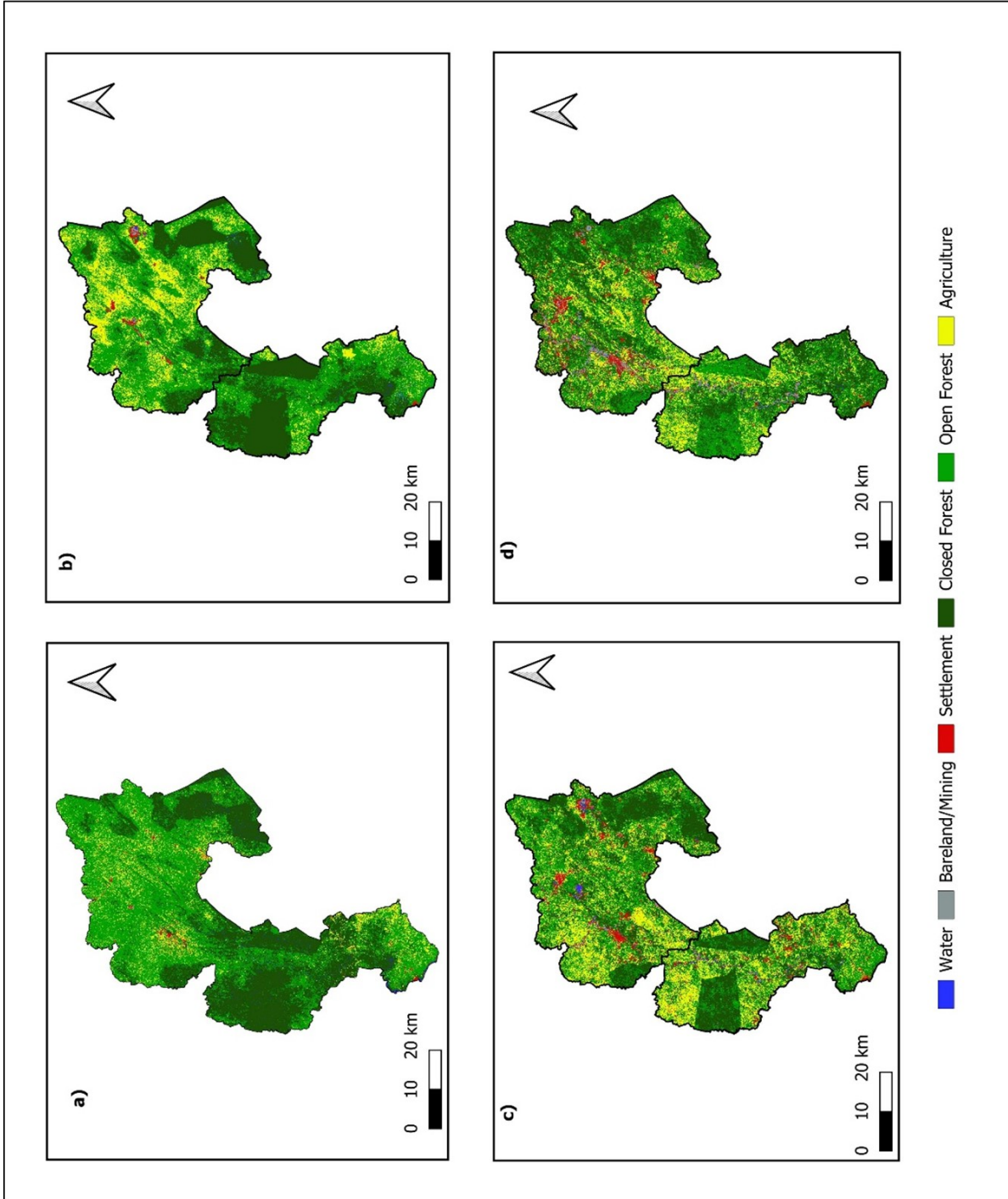


Figure 2: Spatial distribution of LULC classes in the Ankobra River basin for (a) 1986, (b) 2002, (c) 2016, and (d) 2025.

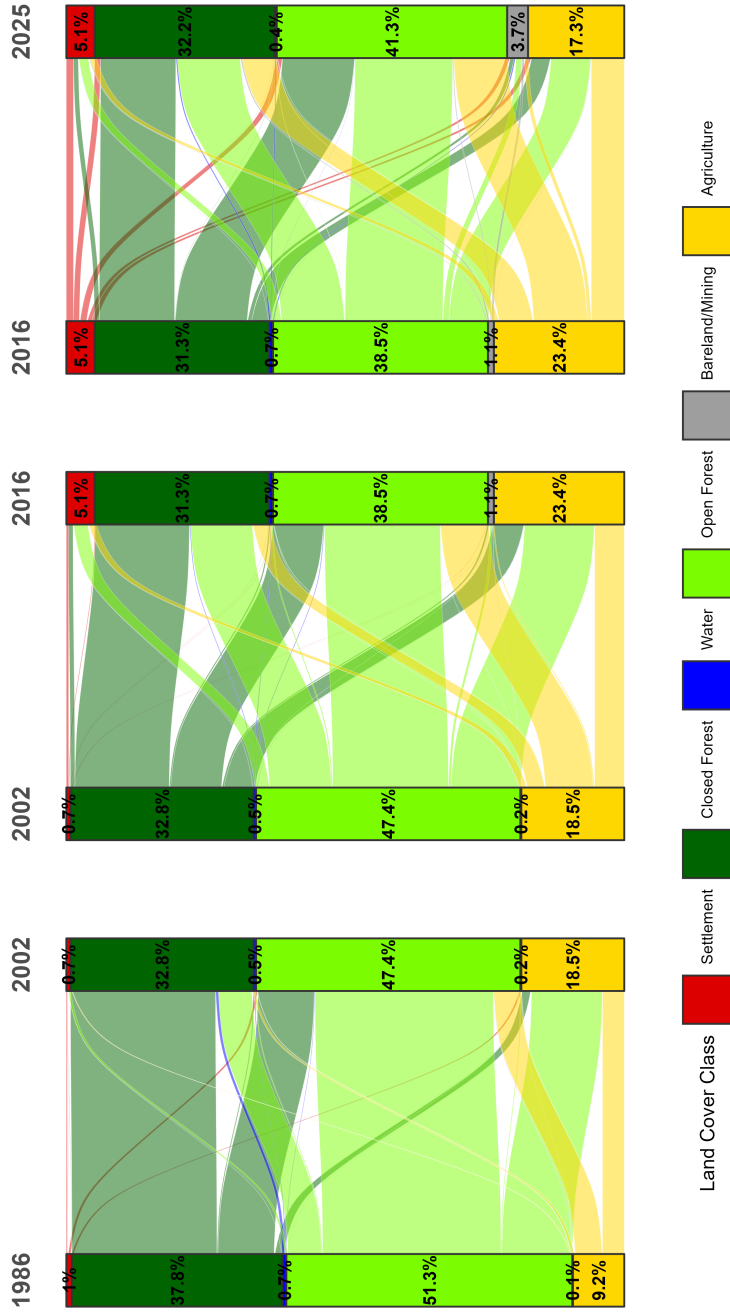


Figure 3: LULC transition pathways in the Ankobra River basin between 1986–2002, 2002–2016, and 2016–2025, shown using Sankey diagrams. Percentages indicate the share of total basin area occupied by each class at the beginning and end of each transition period.

Table 4: LULC classification accuracy assessment across study years

LULC class	1986			2002			2016			2025		
	Precision	Recall	F1-score									
Water	0.85	0.91	0.88	0.88	0.91	0.90	0.81	0.87	0.84	0.93	0.95	0.94
Bareland/Mining	0.82	0.78	0.80	0.85	0.81	0.83	0.77	0.75	0.76	0.89	0.90	0.90
Settlement	0.81	0.85	0.83	0.82	0.85	0.83	0.77	0.82	0.79	0.88	0.91	0.90
Agriculture	0.82	0.84	0.83	0.80	0.86	0.83	0.75	0.79	0.77	0.88	0.90	0.89
Closed Forest	0.90	0.85	0.88	0.89	0.89	0.89	0.87	0.84	0.85	0.92	0.93	0.93
Open Forest	0.90	0.88	0.89	0.95	0.86	0.90	0.93	0.80	0.86	0.99	0.90	0.94
Overall accuracy	85%			86%			81%			92%		

Table 5: Summary statistics of water quality parameters across selected communities

Variable	Ankobra		Bepoh		Dominase		Prestea		Threshold				
	Min	Max	Mean (SD)	Min	Max	Mean (SD)	Min	Max					
pH	6.62	6.79	6.74 (0.04)	6.31	6.83	6.57 (0.18)	6.34	6.65	6.53 (0.10)	5.29	6.55	5.78 (0.53)	6.5–8.5
DO ($mg L^{-1}$)	5.24	5.53	5.32 (0.08)	4.80	6.12	5.42 (0.39)	4.52	6.92	5.47 (0.68)	5.44	6.66	5.97 (0.46)	>5
EC ($\mu S cm^{-1}$)	9933	13250	11233.5 (946.4)	65	94	88.56 (8.93)	110	118	112.36 (2.11)	101	105	102.83 (1.72)	1000
TSS ($mg L^{-1}$)	72	186	133.77 (28.46)	443	978	750.11 (162.45)	1157	2294	1538.18 (298.52)	122	3054	2394.67 (1123.42)	50
TDS ($mg L^{-1}$)	4969	6688	5654.32 (534.24)	44	47	45.89 (1.05)	48	59	55.45 (2.66)	50	52	51.17 (0.98)	500
Turbidity (NTU)	82.3	327.0	147.65 (51.53)	954	1000	994.89 (15.33)	1000	1000	1000.0 (0.0)	338	1000	889.67 (270.26)	5

Note: Reference thresholds are derived from World Health Organization (2017) drinking-water guidelines and Ghana Standards Authority (2021). Values are used for contextual interpretation only.

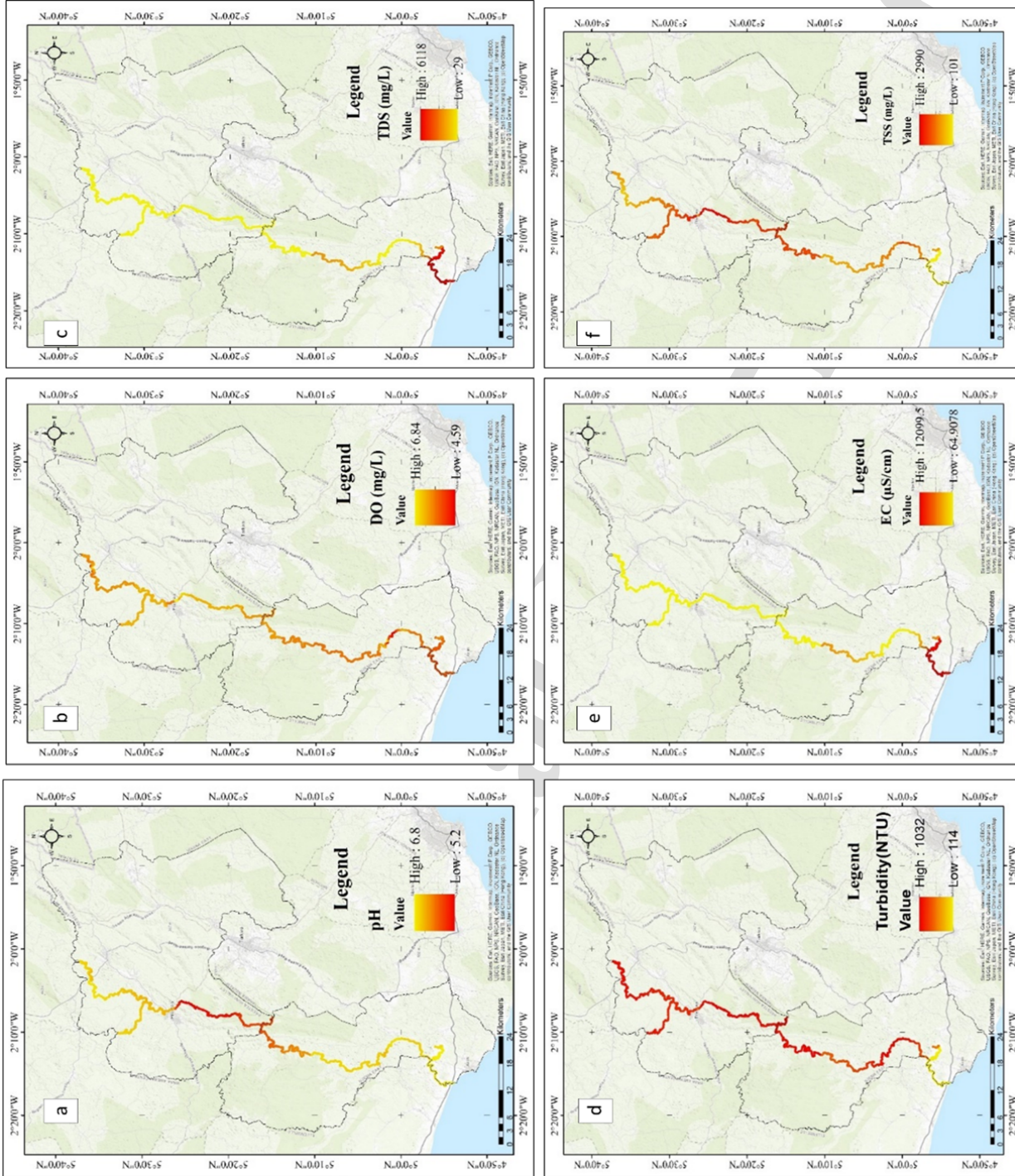


Figure 4: Spatial distribution of interpolated water-quality parameters along the Ankobra River system: (a) pH, (b) dissolved oxygen (DO), (c) total dissolved solids (TDS), (d) turbidity, (e) electrical conductivity (EC), and (f) total suspended solids (TSS). Values represent kriged surfaces derived from field measurements, illustrating longitudinal gradients and localised zones of elevated concentrations along the river network

332 water-quality patterns throughout the basin. Figure 5 shows a clear separation of sampling locations along gradients primarily associated with Bare-
 333 land/Mining and, to a lesser extent, Settlement land use. Bareland/Mining
 334 exhibited the highest marginal contribution among the explanatory variables
 335 ($F = 13.66$, $p < 0.001$), showing strong positive associations with turbidity
 336 and TSS (Table 7). Sampling locations surrounded by higher proportions of
 337 mining-related land cover were consistently aligned with elevated sediment-
 338 related parameters.

340 Forest cover, particularly Closed Forest, was negatively associated with
 341 turbidity and TSS and exerted a statistically significant buffering influence
 342 on water quality ($F = 10.30$, $p < 0.001$). Open Forest and Settlement also
 343 contributed significantly to explaining water-quality variation, although their
 344 effects were weaker ($p < 0.05$), with Settlement showing modest associations
 345 with electrical conductivity (EC) and total dissolved solids (TDS). In con-
 346 trast, Agricultural land cover did not exhibit a statistically significant re-
 347 lationship with any measured water-quality parameter on the spatial scale
 348 examined ($F = 0.36$, $p = 0.728$), indicating limited explanatory power within
 349 the present analytical framework. Monte Carlo permutation tests confirm
 350 that multiple land-use classes contribute significantly to spatial variation in
 351 water quality. Bareland/Mining exhibited the strongest marginal effect, par-
 352 ticularly in relation to sediment-associated parameters, while forest cover
 353 exerted a contrasting buffering influence within the basin.

Table 6: Canonical eigenvalues and variance explained by constrained axes

Axis	Eigenvalue	Variance (%)	Cumulative (%)
RDA1	2.652	44.19	44.19
RDA2	0.114	1.90	46.09
RDA3	0.081	1.34	47.43
RDA4	0.003	0.04	47.47
RDA5	0.001	0.01	47.49
RDA6	< 0.001	< 0.01	< 0.01

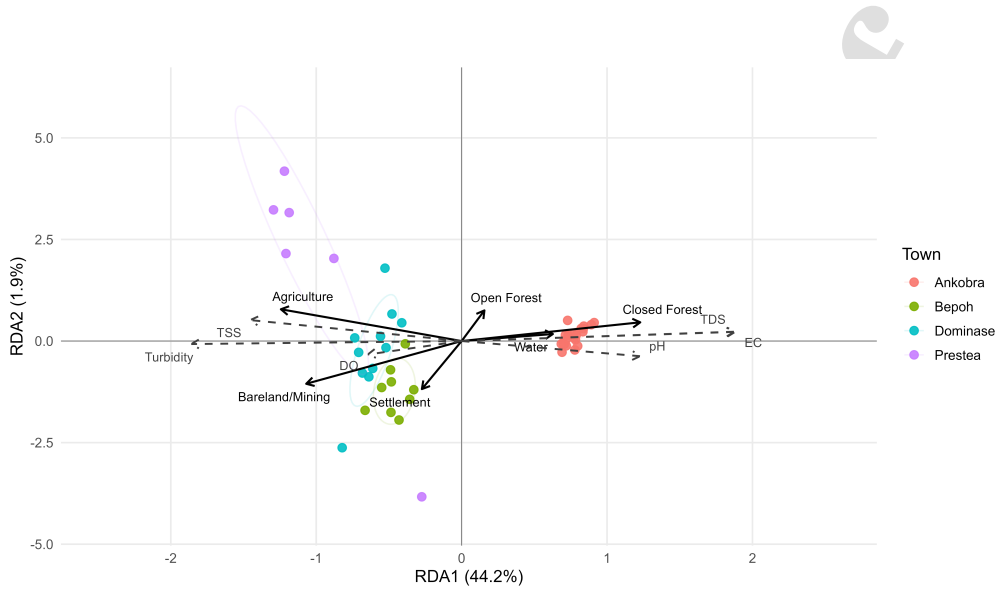


Figure 5: RDA showing land use and land cover influence on water quality

Table 7: Permutation test results (999 permutations) for individual land-use classes

Land-use class	Variance	F-ratio	p-value
Water	0.411	5.35	0.009**
Bareland/Mining	1.050	13.66	< 0.001***
Settlement	0.274	3.57	0.037*
Closed Forest	0.792	10.30	< 0.001***
Open Forest	0.295	3.84	0.026*
Agriculture	0.028	0.36	0.728

*Significant at $p < 0.05$; **highly significant at $p < 0.01$; ***very highly significant at $p < 0.001$.

354 4. Discussion

355 4.1. Land-use transitions, dominant pressures, and sediment-driven river 356 degradation

357 Long-term land-use transitions within the Ankobra River basin have resulted
358 in a landscape characterised by sediment-dominated forms of river degrada-
359 tion, with mining-related disturbance emerging as the dominant pressure

360 shaping spatial variation in water quality (Table 7). This interpretation is
361 based on spatial relationships observed in 2025 and does not imply longitu-
362 dinal causation across the full multi-decadal period.

363 During the study period, Bareland/Mining expanded from a negligible
364 proportion of the basin ($<1\%$, 3 km^2) to more than 100 km^2 . This reflects a
365 transition from a predominantly forested landscape to an increasingly char-
366 acterised by exposed surfaces, hydrologically connected disturbance zones,
367 and intensified human activity. Similar patterns have been documented in
368 mineralised tropical basins, where mining expansion is frequently associated
369 with disproportionate environmental impacts relative to its areal footprint
370 (e.g., Hilson, 2002; Bebbington et al., 2018). In the Ankobra basin, this
371 transformation provides an essential context for interpreting the magnitude
372 and spatial structure of observed water-quality degradation.

373 The spatial patterns of turbidity and total suspended solids (TSS) are
374 consistent with this land-use trajectory and indicate a strong sediment sig-
375 nal linked to mining disturbance. Turbidity values exceeding 1000 NTU
376 and TSS concentrations approaching 3000 mg L^{-1} were observed in river
377 segments downstream of intensive mining activity, particularly within the
378 Prestea–Huni Valley district. By comparison, relatively undisturbed tropical
379 forest rivers typically report turbidity below 2–20 NTU and suspended solids
380 generally $< 5\text{--}50 \text{ mg L}^{-1}$ (Isidore et al., 2019; Njue et al., 2021). The values
381 observed here far exceed thresholds associated with ecological stress and re-
382 duced light penetration (commonly reported above 25–50 NTU) and exceed
383 drinking-water guidelines, which recommend turbidity not exceeding 5 NTU
384 (Franklin et al., 2019; EPA, 2009; Allan, 2004; Hudson-Edwards et al., 2011).
385 Importantly, elevated sediment concentrations were not uniformly distributed
386 across the basin but occurred in spatially clustered zones. This shows that
387 degradation is driven by discrete disturbance hotspots rather than diffuse
388 basin-wide pressure. Spatial concentration reflects the physical mechanisms
389 through which mining affects fluvial systems: clearing vegetation, soil exca-
390 vation, and the creation of pits and waste heaps increase sediment availability
391 and enhance hydrological connectivity between disturbed land surfaces and
392 adjacent channels, particularly during high-intensity rainfall events (Naiman
393 and Decamps, 1997; Hudson-Edwards et al., 2011).

394 Redundancy analysis provides empirical support for linking these sed-
395 iment patterns to specific land-use pressures rather than a simple spatial
396 coincidence. The RDA model explained approximately 47.5% of the total
397 variance in water-quality parameters, with the first canonical axis alone ac-

398 counting for more than 44% of the constrained variation. Approximately
399 52.5% of the total variance remained unexplained. This residual variation
400 likely reflects interacting controls beyond near-stream land-use composition.
401 Geological heterogeneity in the Ankobra basin can influence baseline wa-
402 ter chemistry and sediment characteristics, as variations in lithology and
403 soil composition affect natural turbidity, dissolved constituents, and buffer-
404 ing capacity. In addition, hydrological conditions at the time of sampling
405 influence sediment concentrations, which can vary markedly between base-
406 flow and storm-driven discharge events. Although sampling was conducted
407 during the peak dry season to reduce short-term rainfall effects, instanta-
408 neous flow variability and antecedent conditions cannot be fully controlled in
409 cross-sectional field campaigns. These factors indicate that observed land-use
410 associations operate within a broader hydro-geomorphic context and should
411 be interpreted accordingly.

412 Bareland/Mining exerted the strongest influence on water quality ($F =$
413 13.66 , $p < 0.001$) and showed clear positive associations with turbidity and
414 TSS, confirming that locations surrounded by higher proportions of mining-
415 related land cover were consistently characterised by elevated sediment loads.
416 In contrast, Agricultural land cover did not exhibit statistically significant
417 relationships with any measured water-quality parameter on the spatial scale
418 examined. This finding does not suggest that agriculture is environmentally
419 benign, but rather highlights the scale and parameter-dependence of land-use
420 impacts. Agricultural effects on water quality often manifest through nutri-
421 ent enrichment, pesticide runoff, and fine sediment mobilisation, processes
422 that are strongly modulated by crop type, management practices, and sea-
423 sonal rainfall variability (Foley et al., 2005). In the Ankobra basin, the dom-
424 inance of perennial plantation systems and the focus on sediment-sensitive
425 physico-chemical parameters likely reduce the detectability of agricultural
426 signals within the present analytical framework.

427 Forest cover, particularly Closed Forest, emerged as a statistically sig-
428 nificant buffering influence on river condition, showing strong negative as-
429 sociations with turbidity and TSS ($F = 10.30$, $p < 0.001$). Even within
430 a landscape undergoing rapid extraction transformation, areas retaining a
431 higher canopy cover appear to moderate sediment delivery to the river net-
432 work. This finding is consistent with extensive evidence that forested riparian
433 zones reduce overland flow velocities, improve infiltration, and trap sediments
434 before they reach stream channels, thereby stabilising water quality down-
435 stream (Naiman and Decamps, 1997; Dosskey et al., 2010). The persistence

436 of this buffering effect in the Ankobra basin underscores the disproportionate
437 functional importance of remaining forest patches and riparian vegetation in
438 extractive landscapes, where marginal changes in land cover can yield non-
439 linear responses in river condition.

440 Settlements exhibited weaker but statistically significant associations with
441 electrical conductivity (EC) and total dissolved solids (TDS), suggesting
442 more subtle influences on river chemistry. EC values increased from approx-
443 imately $65 \mu\text{S cm}^{-1}$ in the upstream sections to over $12,000 \mu\text{S cm}^{-1}$ near
444 the estuary, while TDS concentrations exceeded 6000 mg L^{-1} in downstream
445 reaches. While part of this longitudinal gradient likely reflects estuarine
446 processes and saline intrusion as the river approaches the coast, urban and
447 infrastructural contributions—such as wastewater discharge, runoff from im-
448 pervious surfaces, and altered hydrological pathways—may also play a role,
449 particularly where sanitation infrastructure is limited (Paul and Meyer, 2001;
450 Walsh et al., 2005). The co-occurrence of settlement expansion and elevated
451 dissolved constituents highlights the need for caution when attributing chem-
452 ical degradation to single land-use drivers and reinforces the importance
453 of multivariate approaches capable of disentangling overlapping pressures.
454 Given the modest sample size relative to the number of explanatory vari-
455 ables, these findings should be interpreted as indicative of spatial association
456 rather than as definitive parameter estimates.

457 *4.2. Implications for sustainability monitoring and management in extractive* 458 *river basins*

459 The results demonstrate that river degradation in the Ankobra basin is nei-
460 ther spatially uniform nor driven by an undifferentiated set of land-use pres-
461 sures. Instead, sediment-related degradation is strongly concentrated in areas
462 affected by mining-related disturbance, while other land uses exert weaker,
463 more parameter-specific, or scale-dependent influences. This challenges con-
464 ventional basin-wide monitoring approaches that assume homogeneous pres-
465 sure and suggests that sustainability assessments would benefit from more
466 spatially targeted and diagnostically informed strategies.

467 From a monitoring perspective, the dominance of mining-related land
468 cover in explaining turbidity and total suspended solids indicates that surveil-
469 lance and sampling effort should be prioritised along mining corridors and
470 downstream reaches where disturbance is most intense. Uniform sampling
471 designs that distribute limited resources evenly across a basin risk under-
472 representing zones of acute impact while over-sampling relatively stable ar-

473 eas. An attribution-oriented framework allows monitoring programmes to
474 be explicitly aligned with dominant pressures, improving both efficiency and
475 interpretability. In contexts such as southern Ghana, where regulatory agen-
476 cies often face constraints in personnel, funding, and analytical capacity,
477 this prioritisation is important to maintain credible environmental oversight
478 (Bebbington et al., 2018).

479 The results also have direct implications for regulatory enforcement and
480 mitigation strategies. The clear association between Bareland/Mining and
481 extreme sediment loads suggests that sediment control should be a central
482 focus of environmental regulation in the basin, rather than a concern among
483 many. Measures such as the enforcement of buffer zones, containment of
484 spoil material, rehabilitation of abandoned mining pits, and restriction of
485 hydraulic connectivity between disturbed surfaces and river channels are
486 likely to yield disproportionate benefits for water quality relative to more
487 diffuse interventions (Sengupta, 2021). Importantly, the attribution analysis
488 indicates that targeting mining-related disturbance does not imply neglect-
489 ing other land uses, but rather sequencing interventions according to their
490 demonstrated impact. Such prioritisation enhances regulatory legitimacy
491 by linking enforcement actions to observable environmental outcomes rather
492 than to broad or symbolic compliance requirements.

493 The statistically significant buffering effect of forest cover further high-
494 lights the role of landscape configuration in mediating extractive impacts.
495 Even within a heavily disturbed basin, areas that retain Closed Forest are
496 associated with lower sediment loads, underscoring the functional value of
497 forested and riparian vegetation for sustaining water-quality regulation. This
498 supports management approaches that integrate forest conservation and restora-
499 tion into extractive governance frameworks, not as compensatory add-ons
500 but as core components of impact mitigation. Protecting remaining forest
501 patches, strengthening riparian buffers and preventing sequential degradation
502 from forest to open forest to bare disturbance may be particularly effective in
503 slowing or reversing sediment escalation where mining activity persists. Such
504 measures align with broader evidence on nature-based solutions to protect
505 water-quality in disturbed basins (Dosskey et al., 2010).

506 At a broader governance level, the study illustrates how an attribution-
507 oriented sustainability assessment can strengthen decision-making by clarify-
508 ing responsibility and reducing ambiguity around environmental degradation.
509 In many extractive contexts, environmental decline is widely recognised but
510 contested in terms of causation, enabling blame shifting among sectors and

511 undermining accountability. Empirically, distinguishing the relative contri-
512 butions of different land-use pressures as demonstrated in this study pro-
513 vides a more transparent basis for regulatory prioritisation and stakeholder
514 engagement. This is particularly relevant in settings characterised by over-
515 lapping formal and informal governance arrangements, where credibility and
516 evidence-based justification are essential for effective intervention (Scoones,
517 2016; Newell, 2019).

518 Finally, while the findings are grounded in a specific basin, the implica-
519 tions extend beyond the Ankobra context. Many mineralised river basins in
520 the Global South exhibit similar trajectories of forest loss, mining expansion,
521 and fragmented monitoring regimes (e.g., Obodai et al., 2019; Asner et al.,
522 2013; Diringer et al., 2020). The results suggest that sustainability outcomes
523 in such systems depend less on the mere presence of extractive activity than
524 on how land-use transitions unfold, where disturbance is concentrated, and
525 whether residual buffering capacity is maintained.

526 5. Conclusion

527 This study links multi-decadal land-cover change with spatially modelled
528 water-quality data to examine how contemporary extractive land-use pres-
529 sures explain spatial variation in river condition within the Ankobra Basin.
530 The results show that mining-related land disturbance is strongly associ-
531 ated with elevated turbidity and total suspended solids, while forest cover
532 exhibits a contrasting buffering influence on sediment-related parameters.
533 Agriculture and settlement showed weaker and more context-dependent re-
534 lationships with the physico-chemical parameters examined. These findings
535 indicate that water-quality degradation in extractive basins reflects the in-
536 tensity and spatial configuration of specific land-use pressures rather than a
537 uniform landscape change. By explicitly linking land-use composition with
538 observed water-quality variation, the framework provides diagnostic evidence
539 that can support spatially targeted environmental management.

540 The analysis is based on cross-sectional dry-season sampling and near-
541 stream land-use buffers and therefore does not capture seasonal variability,
542 upstream hydrological connectivity, or historical water-quality trends asso-
543 ciated with earlier phases of mining expansion. Extensions of this frame-
544 work could therefore incorporate seasonal sampling, multi-scale buffer evalu-
545 ation, river-network geostatistical approaches, upstream catchment metrics,
546 or complementary process-based modelling to support more robust causal as-

547 sessment. In particular, integrating historical land-cover change trajectories
 548 (e.g., mining expansion during 1986–2002 and 2002–2016) as explicit predic-
 549 tors of contemporary water-quality conditions would strengthen the evalu-
 550 ation of potential legacy sediment effects, provided that temporally aligned
 551 water-quality datasets are available. Integration of trace metal analysis (e.g.
 552 mercury, arsenic, and lead) alongside sediment indicators would further en-
 553 able the assessment of both particulate and dissolved contamination path-
 554 ways associated with gold mining in tropical river systems. Nonetheless,
 555 the approach demonstrated here provides a scalable and replicable means of
 556 linking land-use change to environmental outcomes in extractive landscapes,
 557 prioritising attribution, relevance, and decision support over methodological
 558 novelty alone.

559 References

- 560 Adusei, Y.Y., Quaye-Ballard, J., Adjaottor, A.A., Mensah, A.A., 2021. Spa-
 561 tial prediction and mapping of water quality of owabi reservoir from satel-
 562 lite imageries and machine learning models. *The Egyptian Journal of Re-*
 563 *remote Sensing and Space Science* 24, 825–833. doi:10.1016/j.ejrs.2021.
 564 06.006.
- 565 Allan, J.D., 2004. Landscapes and riverscapes: the influence of land use on
 566 stream ecosystems. *Annu. Rev. Ecol. Evol. Syst.* 35, 257–284.
- 567 Allan, J.D., Manning, N.F., Smith, S.D., Dickinson, C.E., Joseph, C.A.,
 568 Pearsall, D.R., 2017. Ecosystem services of lake erie: Spatial distribution
 569 and concordance of multiple services. *Journal of Great Lakes Research* 43,
 570 678–688. doi:https://doi.org/10.1016/j.jglr.2017.06.001.
- 571 Amoakoh, A.O., Aplin, P., Awuah, K.T., Delgado-Fernandez, I., Moses, C.,
 572 Alonso, C.P., Kankam, S., Mensah, J.C., 2021. Testing the contribution
 573 of multi-source remote sensing features for random forest classification of
 574 the greater Amanzule tropical peatland. *Sensors* 21, 3399. doi:10.3390/
 575 s21103399.
- 576 Amoakoh, A.O., Aplin, P., Rodríguez-Veiga, P., Moses, C., Alonso, C.P.,
 577 Cortés, J.A., Delgado-Fernandez, I., Kankam, S., Mensah, J.C., Nortey,
 578 D.D.N., 2024. Predictive modelling of land cover changes in the Greater
 579 Amanzule peatlands using multi-source remote sensing and machine learn-
 580 ing techniques. *Remote Sensing* 16, 4013. doi:10.3390/rs16214013.

- 581 Armah, F.A., Obiri, S., Yawson, D.O., Pappoe, A.N.M., Akoto, B., 2010.
582 Mining and heavy metal pollution: Assessment of aquatic environments in
583 Tarkwa (Ghana) using multivariate statistical analysis. *Journal of Envi-*
584 *ronmental Statistics* 1, 1–13.
- 585 Asner, G.P., Llactayo, W., Tupayachi, R., Luna, E.R., 2013. Elevated rates
586 of gold mining in the amazon revealed through high-resolution monitoring.
587 *Proceedings of the National Academy of Sciences of the United States of*
588 *America* 110, 18454–18459. doi:10.1073/pnas.1318271110.
- 589 Bebbington, A., Abdulai, A.G., Humphreys Bebbington, D., Hinfelaar, M.,
590 Sanborn, C., 2018. *Governing extractive industries: Politics, histories,*
591 *ideas.* Oxford University Press.
- 592 Belgiu, M., Drăguț, L., 2016. Random forest in remote sensing: A review of
593 applications and future directions. *ISPRS journal of photogrammetry and*
594 *remote sensing* 114, 24–31. doi:10.1016/j.isprsjprs.2016.01.011.
- 595 Cudjoe, K., Nyantakyi, E.K., Borkloe, J.K., Adjei, E.A., Siabi, E.K., Ack-
596 erson, N.O.B., Yeboah, S.I.I.K., Domfeh, M.K., Wezenamo, C.A., Owusu,
597 M., et al., 2023. Assessing livelihood and environmental implications of
598 artisanal and small-scale mining: a case of Akango mining, Nzema East
599 Municipality, Western Region, Ghana. *Environment, Development and*
600 *Sustainability* , 1–28doi:10.1007/s10668-023-04339-x.
- 601 Diring, S.E., Berky, A.J., Marani, M., Ortiz, E.J., Karatum, O., Plata,
602 D.L., Pan, W.K., Hsu-Kim, H., 2020. Deforestation due to artisanal and
603 small-scale gold mining exacerbates soil and mercury mobilization in madre
604 de dios, peru. *Environmental Science & Technology* 54, 286–296. doi:10.
605 1021/acs.est.9b06620.
- 606 Dosskey, M.G., Vidon, P., Gurwick, N.P., Allan, C.J., Duval, T.P., Lowrance,
607 R., 2010. The role of riparian vegetation in protecting and improving
608 chemical water quality in streams. *JAWRA Journal of the American Wa-*
609 *ter Resources Association* 46, 261–277. doi:10.1111/j.1752-1688.2010.
610 00419.x.
- 611 Duncan, A.E., de Vries, N., Nyarko, K.B., 2018. Assessment of heavy metal
612 pollution in the sediments of the River Pra and its tributaries. *Water, Air,*
613 *& Soil Pollution* 229, 272. doi:10.1007/s11270-018-3899-6.

- 614 EPA, 2009. Advice note no. 5: Turbidity in drinking water.
615 URL: [https://www.epa.ie/publications/compliance--enforcement/
616 drinking-water/advice--guidance/Advice-Note-No5.pdf](https://www.epa.ie/publications/compliance--enforcement/drinking-water/advice--guidance/Advice-Note-No5.pdf). version 1,
617 Issued 2 November 2009.
- 618 Foley, J.A., DeFries, R., Asner, G.P., Barford, C., Bonan, G., Carpenter,
619 S.R., Chapin, F.S., Coe, M.T., Daily, G.C., Gibbs, H.K., et al., 2005.
620 Global consequences of land use. *science* 309, 570–574. doi:10.1126/
621 *science*.1111772.
- 622 Franklin, P., Stoffels, R., Clapcott, J., Booker, D., Wagenhoff,
623 A., Hickey, C., 2019. Deriving potential fine sediment at-
624 tribute thresholds for the national objectives framework. URL:
625 [https://environment.govt.nz/assets/Publications/Files/
626 deriving-potential-fine-sediment-attribute-thresholds-for-the-national-objectiv
627 pdf](https://environment.govt.nz/assets/Publications/Files/deriving-potential-fine-sediment-attribute-thresholds-for-the-national-objectives-framework.pdf).
- 628 Ghana Standards Authority, 2021. Water quality – specification for drinking
629 water. URL: [https://www.gsa.gov.gh/wp-content/uploads/2021/03/
630 DGS-175_2021.pdf](https://www.gsa.gov.gh/wp-content/uploads/2021/03/DGS-175_2021.pdf).
- 631 Gorelick, N., Hancher, M., Dixon, M., Ilyushchenko, S., Thau, D., Moore,
632 R., 2017. Google earth engine: Planetary-scale geospatial analysis for
633 everyone. *Remote sensing of Environment* 202, 18–27. doi:10.1016/j.
634 *rse*.2017.06.031.
- 635 Hilson, G., 2002. The environmental impact of small-scale gold mining in
636 ghana: identifying problems and possible solutions. *Geographical Journal*
637 168, 57–72. doi:10.1111/1475-4959.00038.
- 638 Hilson, G., Sauerwein, T., Owen, J., 2020. Large and artisanal scale mine
639 development: The case for autonomous co-existence. *World Development*
640 130, 104919. doi:10.1016/j.worlddev.2020.104919.
- 641 Hudson-Edwards, K.A., Jamieson, H.E., Lottermoser, B.G., 2011. Mine
642 wastes: past, present, future. *Elements* 7, 375–380. doi:10.2113/
643 *gselements*.7.6.375.
- 644 Isidore, F., Cleophas, F., Moh, P.Y., Bidin, K., 2019. A pristine water quality
645 of repeatedly logged forest river in Kawag forest area, Ulu Segama Malua
646 forest reserve, Sabah. *Transactions on Science and Technology* 6, 48–53.

- 647 Jensen, J.R., 2016. *Introductory Digital Image Processing: A Remote Sensing Perspective*. 4th ed., Pearson, Boston.
- 648
- 649 Kuma, J.S., Younger, P.L., 2004. Water quality trends in the Tarkwa gold-
650 mining district, Ghana. *Bulletin of Engineering Geology and the Environ-*
651 *ment* 63, 119–132. doi:10.1007/s10064-004-0227-8.
- 652 Li, J., Heap, A.D., 2014. Spatial interpolation methods applied in the en-
653 vironmental sciences: A review. *Environmental Modelling & Software* 53,
654 173–189. doi:10.1016/j.envsoft.2013.12.008.
- 655 Ma, C., Sun, W., Yang, Z., Wang, J., Zhou, L., 2025. Spatiotemporal vari-
656 ations in land use impacts on river water quality in a mountain-to-plain
657 transitional basin in arid region of northern China. *Journal of Contaminant*
658 *Hydrology* 271, 104542. doi:10.1016/j.jconhyd.2025.104542.
- 659 Minerals Commission of Ghana, n.d. Ghana mining repository. <https://ghana.revenuedev.org>. Accessed March 2026.
- 660
- 661 Naiman, R.J., Decamps, H., 1997. The ecology of interfaces: riparian zones.
662 *Annual review of Ecology and Systematics* 28, 621–658. doi:10.1146/
663 *annurev.ecolsys.28.1.621*.
- 664 Newell, P., 2019. *Trasformismo or transformation? the global political econ-*
665 *omy of energy transitions*. *Review of international political economy* 26,
666 25–48. doi:10.1080/09692290.2018.1511448.
- 667 Njue, N., Gräf, J., Weeser, B., Rufino, M.C., Breuer, L., Jacobs, S.R., 2021.
668 *Monitoring of suspended sediments in a tropical forested landscape with*
669 *citizen science*. *Frontiers in Water* 3, 656770. doi:10.3389/frwa.2021.
670 656770.
- 671 Obodai, J., Adjei, K.A., Odai, S.N., Lumor, M., 2019. Land use/land
672 cover dynamics using landsat data in a gold mining basin-the Ankobra,
673 ghana. *Remote Sensing Applications: Society and Environment* 13, 247–
674 256. doi:10.1016/j.rsase.2018.10.007.
- 675 Opoku, M.E., Salkushu, W., Hammond, F., 2017. A hybrid image clas-
676 sification approach to monitoring lulc changes in the mining district of
677 prestea-huni valley, Ghana. *Journal of Environment and Earth Science* 7,
678 1–10.

- 679 Osei, J.D., Arhin, E., Twumasi, Y.A., Yevugah, L.L., Boakye, L., Damoah-
680 Afari, P., Saah, D., Coffie, P.B., 2024. Poisoned for gold: Assessing the spa-
681 tial extent of heavy metal contamination within the Tutua-Bura-Angoben
682 shelter belt forest reserve in Ghana. *Watershed Ecology and the Environ-*
683 *ment* 6, 146–154. doi:10.1016/j.wsee.2024.08.001.
- 684 Paul, M.J., Meyer, J.L., 2001. Streams in the urban landscape. *Annual*
685 *review of Ecology and Systematics* 32, 333–365. doi:10.1146/annurev.
686 *ecolsys.32.081501.114040*.
- 687 Scoones, I., 2016. The politics of sustainability and development. *An-*
688 *ual Review of Environment and Resources* 41, 293–319. doi:10.1146/
689 *annurev-environ-110615-090039*.
- 690 Sengupta, M., 2021. *Environmental Impacts of Mining: Monitoring, Restora-*
691 *tion, and Control*. CRC Press, Boca Raton, FL.
- 692 Turnhout, E., Metzger, T., Wyborn, C., Klenk, N., Louder, E., 2020. The
693 politics of co-production: participation, power, and transformation. *Cur-*
694 *rent opinion in environmental sustainability* 42, 15–21. doi:10.1016/j.
695 *cosust.2019.11.009*.
- 696 Walsh, C.J., Roy, A.H., Feminella, J.W., Cottingham, P.D., Groffman, P.M.,
697 Morgan, R.P., 2005. The urban stream syndrome: current knowledge and
698 the search for a cure. *Journal of the North American Benthological Society*
699 24, 706–723. doi:10.1899/04-028.1.
- 700 Wiafe, S., Awuah Yeboah, E., Boakye, E., Ofori, S., 2022. Environmental
701 risk assessment of heavy metals contamination in the catchment of small-
702 scale mining enclave in Prestea Huni-Valley District, Ghana. *Sustainable*
703 *Environment* 8, 2062825. doi:10.1080/27658511.2022.2062825.
- 704 World Health Organization, 2017. *Guidelines for Drinking-water Quality*. 4th
705 ed., World Health Organization, Geneva. URL: [https://www.who.int/
706 publications/i/item/9789241549950](https://www.who.int/publications/i/item/9789241549950).

707 **Appendix A. LULC transition matrices**

708 Appendix Table A1 presents the LULC transition matrices for the Ankobra
709 River basin, showing area-based transitions (km²) between LULC classes

710 for the periods 1986–2002, 2002–2016, and 2016–2025. The matrices provide
711 detailed quantitative support for the dominant transition pathways discussed
712 in the Results section and underpin the long-term land-use change patterns
713 illustrated in Figure 3.

Table A1: LULC transition matrices for the Ankobra River basin (km²)

Transitions to 2002									
From / To	Water	Bareland/Mining Settlement	Closed Forest	Open Forest	Agriculture				
Water	3.45	0.01	4.75	4.26	0.57				
Bareland/Mining Settlement	0.01	0.23	0.17	3.69	0.85				
Closed Forest	0.10	0.16	1.18	11.26	3.59				
Open Forest	13.60	0.15	750.85	173.22	9.99				
Agriculture	2.57	1.81	290.72	924.04	138.64				
	0.27	0.93	44.39	365.87	112.69				
Transitions to 2016									
From / To	Water	Bareland/Mining Settlement	Closed Forest	Open Forest	Agriculture				
Water	3.47	0.85	6.66	5.66	1.70				
Bareland/Mining Settlement	1.03	1.27	10.17	12.58	5.52				
Closed Forest	0.50	1.68	22.56	72.64	37.78				
Open Forest	3.51	0.76	487.91	319.56	88.92				
Agriculture	3.47	0.25	262.21	598.80	246.82				
	1.20	0.15	159.24	360.64	153.11				
Transitions to 2025									
From / To	Water	Bareland/Mining Settlement	Closed Forest	Open Forest	Agriculture				
Water	4.64	1.54	1.71	1.42	0.63				
Bareland/Mining Settlement	6.23	11.58	19.93	30.77	18.36				
Closed Forest	0.93	4.47	24.35	47.97	33.98				
Open Forest	6.23	7.54	390.09	325.08	174.96				
Agriculture	1.24	4.61	371.47	503.83	277.69				
	0.43	1.70	97.15	204.77	170.40				

Values represent area transitions between LULC classes (km²). Rows indicate source classes and columns indicate destination classes for each time period.

714 *Supplementary accuracy assessment outputs*

715 This appendix provides supplementary materials supporting the LULC clas-
 716 sification and change analysis presented in the main text. Figure A1 presents
 717 the full confusion matrices for each classification year (1986, 2002, 2016, and
 718 2025), illustrating class-level agreement between reference data and model
 719 predictions. These matrices underpin the summary accuracy metrics re-
 720 ported in Section 3.2 and Table 4 and are included here to ensure trans-
 721 parency in the classification performance assessment.

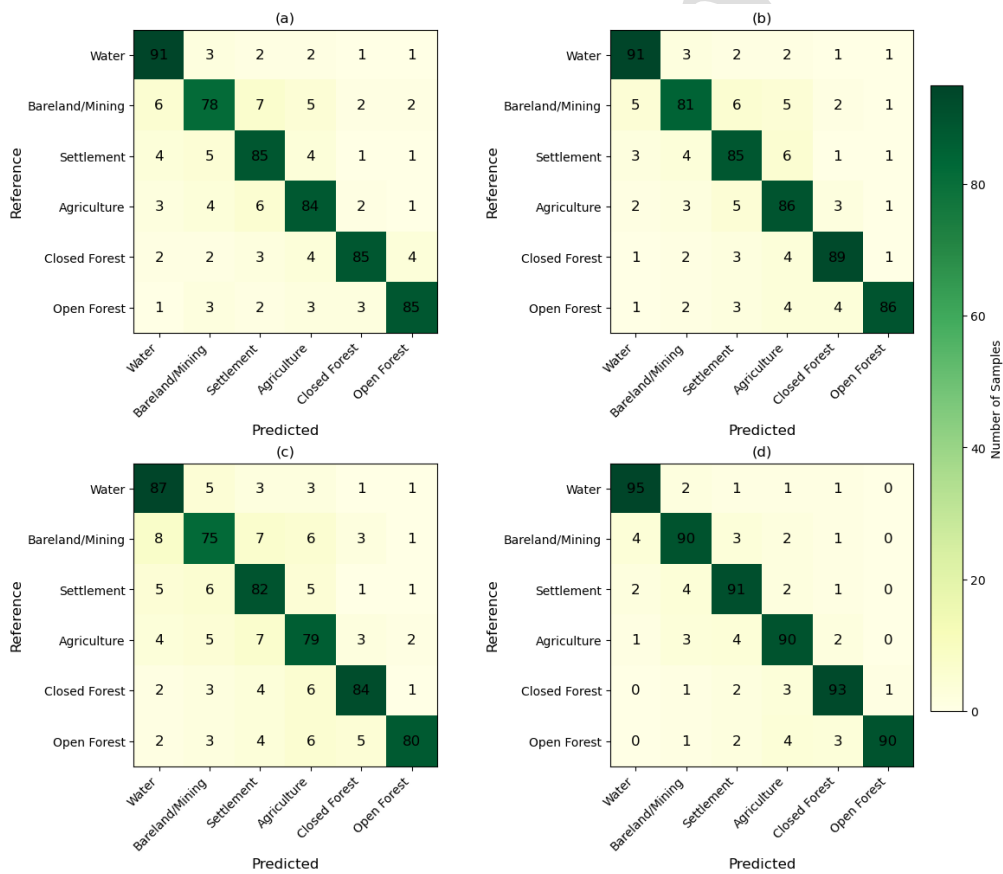


Figure A1: Confusion matrices for LULC classifications for (a) 1986, (b) 2002, (c) 2016, and (d) 2025. Rows represent reference classes and columns represent predicted classes. Cell values indicate the number of validation samples per class.

722 *Appendix A.1. Accuracy-adjusted land-cover area estimates*

723 To account for classification uncertainty and provide statistically robust es-
724 timates of land-cover extent, accuracy-adjusted area estimates were derived
725 for each LULC class and study year following standard post-classification
726 adjustment procedures. Table A2 reports the adjusted area estimates and
727 corresponding percentage share of the total basin area, together with 95%
728 confidence intervals. These estimates complement the mapped area statistics
729 presented in Table 3 by quantifying uncertainty associated with classification
730 error and enabling more reliable comparison of land-cover change across time.

Table A2: Area-adjusted land-cover estimates and corresponding percentage share of the total basin area, with 95% confidence intervals, for each land-cover class across the study periods.

Class	1986			2002			2016			2025						
	Area (km ² ± CI)	Share (% ± CI)														
Water	84.66 ±	2.93 ±	50.89 ±	1.76 ±	98.96 ±	3.42 ±	26.97 ±	0.93 ±	54.94	1.90	38.74	1.34	50.29	1.74	19.10	0.66
Bareland/Mining	85.97 ±	2.97 ±	71.81 ±	2.48 ±	131.58 ±	4.55 ±	148.22 ±	5.13 ±	59.16	2.05	51.33	1.77	58.70	2.03	41.01	1.42
Settlement	140.08 ±	4.84 ±	123.29 ±	4.26 ±	258.11 ±	8.93 ±	209.52 ±	7.25 ±	71.42	2.47	63.73	2.20	68.38	2.36	51.23	1.77
Closed Forest	986.55 ±	34.11 ±	893.86 ±	30.91 ±	831.72 ±	28.76 ±	900.56 ±	31.14 ±	97.39	3.37	85.75	2.97	94.53	3.27	70.65	2.44
Open Forest	1290.61 ±	44.63 ±	1269.46 ±	43.90 ±	999.37 ±	34.56 ±	1145.53 ±	39.61 ±	± 108.37	3.75	± 92.11	3.19	90.37	3.12	± 67.11	2.32
Agriculture	304.15 ±	10.52 ±	482.70 ±	16.69 ±	572.07 ±	19.78 ±	461.14 ±	15.95 ±	63.24	2.19	48.73	1.68	62.50	2.16	37.45	1.29

Area-adjusted estimates were derived using accuracy-adjusted area estimation methods to account for classification uncertainty. Confidence intervals represent 95% uncertainty bounds around each estimate.

Author Credit Statement

Vincent Adjei: Conceptualisation, Methodology, Data curation, Formal analysis, Writing - original draft.

Lawson Mensah: Field investigation, Data curation, Laboratory analysis, Supervision, Writing - review & editing.

Alex Owusu Amoakoh: Conceptualisation, Methodology, Supervision, Formal analysis, Writing - review & editing.

Mary Antwi: Field investigation, Methodology, Supervision, Writing - review & editing.

Gideon Nkrumah: Field investigation, Data curation, Writing - review & editing.

Isaac Stanislav Essah: Methodology, Writing - review & editing.

Frederick Gyan: Laboratory analysis, Data curation, Writing - review & editing.

Vera Aseye Ekor: Field investigation, Data curation, Writing - review & editing.

Godfred Adu Boateng: Conceptualisation, Writing - review & editing.

Declaration of interests

1. Declaration of interests

The authors declare that they have no known competing financial interests or personal relationships that could have appeared to influence the work reported in this paper.

The authors declare the following financial interests/personal relationships which may be considered as potential competing interests:

NA

2. Contributions

Each author declares substantial contributions through the following:

- (1) the conception and design of the study, or acquisition of data, or analysis and interpretation of data,
- (2) drafting the article or revising it critically for important intellectual content,

Please indicate for each author the author contributions in the text field below. Signatures are not required.

Vincent Adjei contributed to the conception and design of the study, data analysis and interpretation, and drafting of the manuscript. Lawson Mensah contributed to data acquisition through field and laboratory work and to manuscript revision. Alex Owusu Amoakoh contributed to the conception and design of the study, data analysis and interpretation, supervision, and critical revision of the manuscript. Mary Antwi contributed to field investigation, methodological input, supervision, and manuscript revision. Gideon Nkrumah, Frederick Gyan, and Vera Aseye Edor contributed to data acquisition and manuscript revision. Isaac Stanislav Essah contributed to methodological development and manuscript revision. Godfred Adu Boateng contributed to study conception and manuscript revision.

3. Approval of the submitted version of the manuscript

Please check this box to confirm that all co-authors have read and approved the version of the manuscript that is submitted. Signatures are not required.